VO_2/ZnO bilayer films with enhanced thermochromic property and durability for smart windows

Zhaoda Fang [a], Shouqin Tian [a,*], Bin Li [a], Qiufen Liu [a], Baoshun Liu [a], Xiujian Zhao [a], Gopinathan Sankar [b]

[a] State Key Laboratory of Silicate Materials for Architectures, Wuhan University of Technology (WUT), No. 122, Luoshi Road, Wuhan 430070, P. R. China

[b] Department of Chemistry, Materials Chemistry Centre, University College London, 20 Gordon St., London WC1H 0AJ, UK

*Corresponding author. Tel.: +86-027-87652553; Fax: +86-027-87883743.

E-mail address: tiansq@whut.edu.cn (S. Tian)

Abstract:

VO_2 films are widely considered as one of the most suitable material to act as smart windows. Although this system is able to function, the durability of the film has been an issue as the surface of the films may oxidize by converting V^{4+} to V^{5+}. To overcome this problem, attempt is made to coat the VO_2 film with ZnO, which can assist by creating a resistance layer to prevent further oxidation of VO_2. Here, VO_2/ZnO bilayer film was prepared by a facile method comprised of spin-coating and dip-coating process and shows excellent durability, and in particular. the solar modulation efficiency (ΔT_{sol}) maintaining ca 89.9% (from 17.8% to 16.0%) after 300 days in a humid environment, however, the ΔT_{sol} of pure VO_2 film is decreased from 11.8% to 4.1%. Also, the VO_2/ZnO bilayer exhibits an enhanced thermochromic property of visible transmittance (T_{lum}=55.7±2.1%) and ΔT_{sol} (17.1±1.4%) which is 1.49 times higher than that of pure VO_2 film (ΔT_{sol} = 11.5±0.4%). The enhancement in the thermochromic performance and durability is probably attributed to the anti-reflection and protection of ZnO layer. Therefore, this work can provide an effective way to optimize thermochromic property for practical application of VO_2-based smart windows.

Keywords: VO_2/ZnO bilayer film, durability, thermochromic, smart windows

1. Introduction:

Recent years, energy crisis has been one of the greatest challenges faced by human society and therefore the research on energy saving has attracted more attention. It is reported that 40% of total energy consumption in the world comes from energy consumption in buildings [1], and the use of temperature controlling device in terms of cooling and heating accounts for 40-60% of a building's total energy consumption [2]. At the same time, the normal window also results in a large energy wastage due to its poor thermal insulation performance. To reduce the energy consumption, the smart window with good solar heat control ability in response to an external stimulus such as electricity [3-5], reactive gases [6], light [7,8] or heat [9-11] are attracting much interests. Thermochromic windows are one of the most typical system widely considered for solar energy regulation. Vanadium dioxide (VO_2) is one of the ideal material for thermochromic windows, widely investigated, because it undergoes a reversible metal to insulator phase transition (MIT) at the critical temperature (T_c) of 68 °C (bulk) accompanied by a dramatic change in the near-infrared (NIR) region which is transparent to NIR light below T_c while translucent to NIR light above T_c [12].

At present, most of the work on VO_2-based thermochromic film for smart windows have been focused on the improvement in its thermochromic performance such as increasing luminous transmittance (T_{lum}) [11,13,14], enhancing solar regulation efficiency (ΔT_{sol}) [13-17] and reducing phase transition temperature (T_c) [18-20]. Whilst these aspects are very important, at the same time the durability of VO_2-based smart window is less investigated as it is also a vital property for long term usage. As we know, VO_2 particles in films will be naturally oxidized by the oxygen in air to form more stable V_2O_5 on their surface [21-23], leading to the deterioration of MIT property [24,25]. In order to improve the durability of VO_2, core-shell structures have been investigated recently with VO_2 cores surrounded by shells comprised of SiO_2 [23,26,27], TiO_2 [28], AlO_x [22], ZnO [29], MgF_2 [30] serving as chemical protective barrier. Although this method can enhance the durability of VO_2 obviously, it does not meet the needs for our daily life operations as their preparation process is very complicated. In addition, the oxidation process of VO_2 in air, in these systems has not been addressed clearly. Therefore, it is of great importance to understand the role

of protective layer with VO_2 that may prevent oxidation in air and find a facile way to enhance the durability of VO_2 based films.

In this work, we report the preparation of a porous VO_2/ZnO bilayer film (ZnO film used as buffer layer, anti-reflective layer and protection layer) by a facile method involving of spin-coating and dip-coating processes. The bilayer film prepared by these methods shows excellent durability that the ΔT_{sol} keeps 89.9% (from 17.8% to 16.0%) after 300 days in a humid environment while ΔT_{sol} of pure VO_2 film is obviously decreased from 11.8% to 4.1%. In addition, the surface compositions of VO_2 film and VO_2/ZnO bilayer film after 300 days were characterized by XPS to investigate the oxidation process of VO_2. The enhancement in the durability of VO_2/ZnO bilayer film is probably attributed to the electron transfer from ZnO to VO_2. In addition, the obtained VO_2/ZnO bilayer film exhibited excellent thermochromic performance with ΔT_{sol} of 17.1% and T_{lum} of 55.7%, which is better than the VO_2-based film in most previous works.

2. Experimental Section

2.1. The preparation of VO_2 nanoparticles

All reagents were purchased from the Sinopharm Chemical Reagent Co., Ltd., and were used without further purification. According to our previous work [20,31], porous VO_2 nanocrystals were prepared by the following simple hydrothermal method with cotton as macro template. 0.4 g (0.0022 mol) of vanadium pentoxide (V_2O_5) and 0.832 g (0.0066 mol) of oxalic acid were dissolved in 30 mL of deionized water, and then 30 mL of ethylene glycol was added to increase the viscosity of the solution. As the cotton degrades the acidic solutions, 1 mL of ammonia was added to adjust the pH to *ca*. 7. The solution and 0.5 g of cotton were transferred to a 100 mL Teflon-lined stainless-steel autoclave. The autoclave was maintained at a temperature of 180 °C for 20 h and then cooled to room temperature naturally. The black product was separated and washed with water and ethanol, and then dried in air at 60 °C for 20 h. In order to remove the template to get porous powders, the product was heated in air at 400 °C for 1 h (ramp rate *ca*. 3 °C min^{-1}). Finally, 0.2 g of the obtained mesoporous V_2O_5 and 0.1 g of NH_4HCO_4 were placed in a vacuum tube furnace for 450 °C for 30 min. Ammonia gas produced from the decomposition of NH_4HCO_3 reduced V_2O_5 to VO_2 and thus the porous VO_2 nanocrystals can be obtained. The

porous VO_2 structure was detailed characterized by SEM, TEM, HRTEM and BET methods in our previous works [20, 31]. In addition, the preparation process showed good repeatability. In this sense, the obtained porous VO_2 structure was not characterized by the above methods here.

2.2. The preparation of ZnO film

According to our previous work [32], the ZnO films were prepared on the glass surface by dip-coating method. 5.4876 g of zinc acetate dihydrate ($Zn(CH_3COO)_2 \cdot 2H_2O$) was dissolved in 50 mL of methanol. Then 1.5 mL of ethanolamine was added into the above solution and the solution was stirred for 24 h to get a transparent sol. The sol was used to prepare a film on the glass surface by dip-coating method with the dipping time of 3 min. The film was put on the hot plate at 350 °C for 60 min. After dip coating for three times, the film was heated in the furnace at 350 °C for 60 min to get transparent ZnO film.

2.3. The preparation of VO_2/ZnO bilayer film

0.5 g of VO_2 nanoparticles were dispersed in ethanol that contained 0.25 g of PVP by grinding for 8 h. This solution was then sonicated to ensure good mixing. After centrifugation at 8000 rpm, a suspension was formed. This suspension was then uniformly cast onto the above ZnO film by spin-coating at the speed of 500 rpm for 10 s and then 1000 rpm for 20 s. Finally, the ethanol was removed by drying in an oven at 80 °C for 1 min, yielding VO_2/ZnO bilayer film.

2.4. Characterization

The crystalline phase of the obtained film was determined by X-ray diffraction (XRD, D8Advance, CuKα, λ = 0.154178 nm produced under a 3 kW output power). The morphology and the thicknesses of films were examined by a field emission scanning electron microscopy (SEM, JSM-5610LV, Japan). The surface structure of the films was characterized by a Raman measurement (Raman，LABRAN HR Evolution，HORIBA). The surface compositions of the films were determined by X-ray photoelectron spectroscopy (XPS, ESCALAB 250Xi, Thermo Fisher). The thermochromic properties of the films from 300 to 2500 nm was measured with ultraviolet–visible–near-infrared spectrophotometer (UV–Vis–NIR, UV-3600) at the temperature of 20 °C and 90 °C, respectively.

The integrated luminous transmittance (T_{lum}, 380-780 nm) and solar transmittance (T_{sol}, 300−2500 nm) were obtained from the following equation.

$$T_{lum/sol} = \int \varphi_{lum/sol}(\lambda)T(\lambda)d\lambda / \int \varphi_{lum/sol}(\lambda)d\lambda$$

Where, $T(\lambda)$ denotes film transmittance at a wavelength (λ), $\varphi_{lum}(\lambda)$ is the standard luminous efficiency function for the photopic vision of human eyes, $\varphi_{sol}(\lambda)$ is the solar irradiance spectrum for air mass 1.5 corresponding to the sun standing 37° above the horizon [33,34]. ΔT_{sol} is attained from:

$$\Delta T_{sol} = T_{sol}(20\ ^{\circ}C) - T_{sol}(90\ ^{\circ}C)$$

3. Results and discussion

3.1. The phase compositions of VO_2/ZnO bilayer film

To confirm the phases presented in the obtained bilayer film, XRD characterization was carried out at room temperature and the result is shown in Fig. 1. It can be seen that some diffraction peaks belong to ZnO (JCPDS no.5-664) and the other diffraction peaks are indexed to M-phase VO_2 (JCPDS no. 44-252), indicating that the obtained film is composed of ZnO and VO_2. Furthermore, there are no diffraction peaks which can be indexed to other compounds, implying that there are no other compounds in the bilayer film; the large amorphous background is from glass substrate.

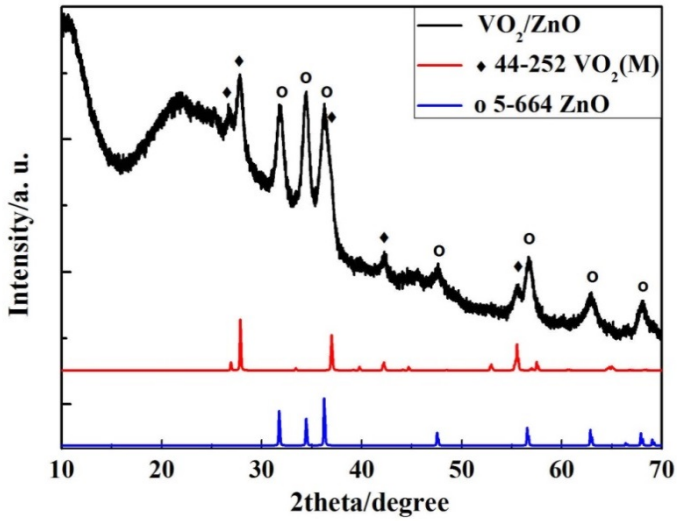

Fig. 1. XRD patterns of the obtained bilayer film.

Fig. 2a shows the representative cross-section SEM image for the bilayer film, where a bilayer structure can be clearly observed. The thickness of top VO_2 layer is estimated to be 1150 nm The bottom layer with a thickness of 280 nm is ZnO layer. On the top of the VO_2 layer, there is another thin layer which color is similar to that of ZnO layer. The thin film exhibited dozens of nanometers in the thickness but is not uniform like the ZnO layer. Because SEM images were taken after the prepared film was kept for several days, some ZnO nanocrystals were formed on the top layer after the film preparation processes The cross-section SEM image for VO_2 film is presented in Fig. 2b. It can be seen that the film thickness is about 1080 nm, which is close to the thickness of VO_2 layer in bilayer film. In addition, the ZnO film is uniform and compact, but the VO_2 layer is uneven. This is because that VO_2 layer is composed of VO_2 particles and PVP.

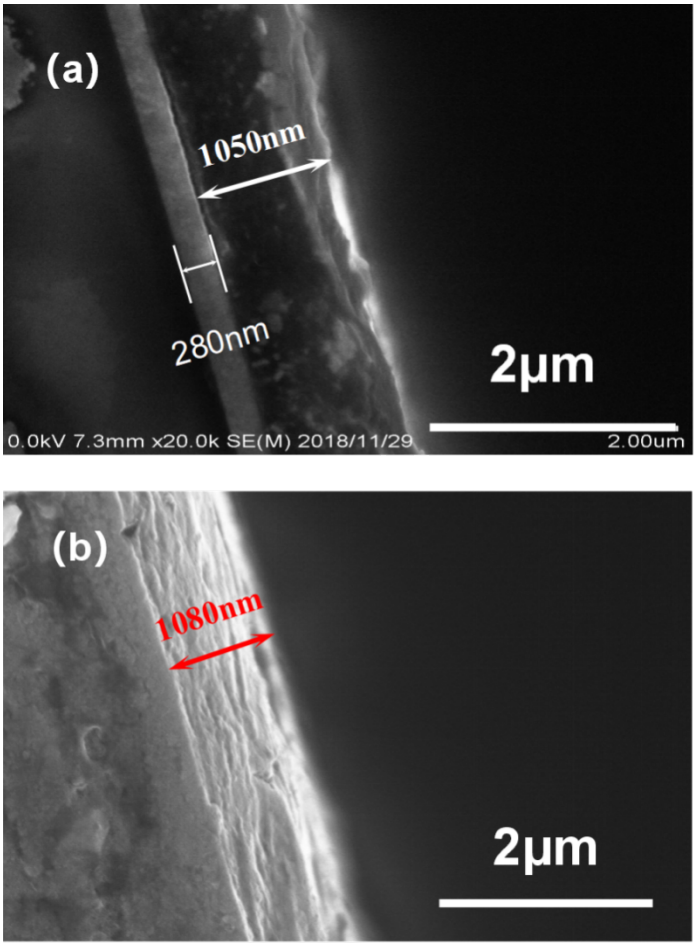

Fig. 2. Cross-section SEM images of (a) VO_2/ZnO bilayer film and (b) VO_2 film.

To determine the elemental composition of films, EDS measurements were employed and the results are shown in Fig. 3a, b. It can be seen that V, O and Zn elements are uniformly dispersed in

the bilayer film and similarly the V and O elements are also distributed evenly in the VO_2 film. The SEM image for the surface morphology of the bilayer film is presented in Fig. 3c, the white dots are likely VO_2 grains. Fig. 3d presents the solar transmittances of the VO_2/ZnO bilayer film at different testing temperatures. Obviously, the VO_2/ZnO bilayer film exhibits high luminous transmittance (T_{lum}) of 59.9% at 20 °C and a large difference in the solar transmittance (ΔT_{sol}) of 19.6% between 20 °C and 90 °C. Such thermochromic properties are more excellent than that of most previous works [21-23,27,29,31,33-35], and detailed performance are summarized in Table 1.

Table 1 Comparison between this work with some recently reported VO_2 based films

VO_2 films	T_{lum} (%)	ΔT_{sol} (%)	Ref.
VO_2/ZnO bilayer film	59.9	19.6	This work
ZnO/VO_2 nanofilm	50.3	12.2	21
VO_2/Al-O core-shell structure	-	9.62	22
VO_2@SiO_2/PU composite film	55.3	7.5	23
VO_2@SiO_2 composite film	71.02	14.3	27
VO_2@ZnObased film	51.0	19.1	29
Mesoporous VO_2 based film	56.0	12.9	31
Double side VO_2 film	68.2	11.7	33
3D ordered macroporous VO_2 films	71.7	4.7	34
$V_{1-x}W_xO_2$/WO_3 composite based films	60.8	9.7	35

"-" denotes not mentioned

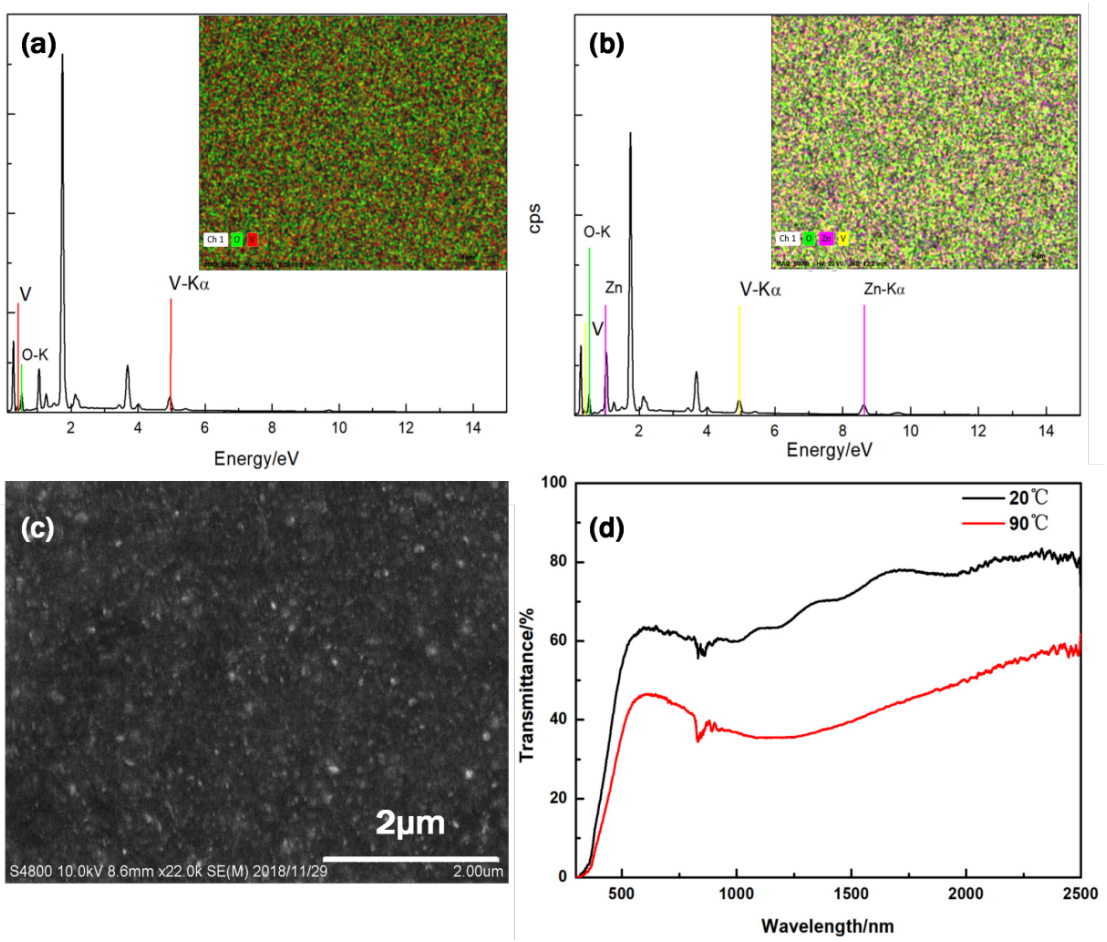

Fig. 3. EDS spectra of (a) VO_2 film and (b)VO_2/ZnO bilayer film, the inset is element mapping of the films, (c) the SEM image of VO_2/ZnO bilayer film, and (d) transmittance spectra in the range from 300 nm to 2500 nm for the VO_2/ZnO film at 20 °C and 90 °C respectively.

3.2. Optical properties of VO_2/ZnO bilayer film

To determine the repeatability and reproducibility of preparing VO_2/ZnO bilayer film, VO_2 film samples were prepared again, three more times, using identical procedures. The calculated optical performance (T_{lum} and ΔT_{sol}) is summarized in Table 2. It can be seen that the luminous transmittance of bilayer film is not as good as that of VO_2 films, ranging from 52.0% to 58.0%, and the average luminous transmittance is 55.7% (20 °C), while the average luminous transmittance of VO_2 film is 59.2%. Nevertheless, the solar modulation efficiency is improved and the determined average solar modulation efficiency is 17.1% which indicates that ΔT_{sol} of bilayer films was improved by 49.0% compared with that of VO_2 film (ΔT_{sol}=11.5%). The results suggest that the bilayer film exhibits enhanced solar modulation efficiency with remaining high visible

transmittance.

Table 2 Optical properties of different VO_2/ZnO bilayer films and VO_2 films prepared by the same method.

sample	T_{lum} (%)		T_{sol} (%)		ΔT_{sol} (%)
	20 °C	90 °C	20 °C	90 °C	
bilayer film S1	58.7	45.6	56.7	40.7	16.0
bilayer film S2	56.1	48.3	57.5	41.7	15.8
bilayer film S3	52.1	41.9	52.4	35.0	17.4
bilayer film S4	55.9	39.5	53.7	34.4	19.3
average±σ	**55.7±2.1**	**43.8±3.4**	**55.1±2.1**	**38.0±3.3**	**17.1±1.4**
VO_2 film S1	60.4	55.2	58.4	46.6	11.8
VO_2 film S2	55.9	54.5	57.9	46.2	11.7
VO_2 film S3	61.3	59.6	62.8	51.9	10.9
average±σ	**59.2±2.4**	**56.4±2.3**	**59.7±2.2**	**48.2±2.6**	**11.5±0.4**

In order to further investigate the thermochromic property of VO_2/ZnO bilayer film, the transmittance spectra were obtained at different testing temperatures from 20 °C to 90 °C (interval was 10 °C) for VO_2 film and VO_2/ZnO bilayer film and shown in Fig. 4. It can be seen in Fig. 4a that the near-infrared transmittance of porous VO_2 films (>780 nm) remained almost unchanged from 20 °C to 50 °C (> 780 nm) but decreased significantly when the temperature was increased further up to 60 °C. This was probably due to the MIT transition of VO_2 at 68 °C. In contrast, Fig. 4b shows the near-infrared transmittance of VO_2/ZnO bilayer film (>780 nm) which decrease gradually from 20 °C to 90 °C, there is no abrupt change that seen in mono layer VO_2 films observed for the bilayer film. In addition, the difference at the visible light region of bilayer film is much larger than VO_2 film, which indicates that the structure of bilayer film may have a certain ability to regulate the visible transmittance at different temperatures. The specific optical performance data is shown in Table 3. It can be seen that ΔT_{sol} of VO_2 film is only 1.4% at 50 °C, which indicates that there are nearly no differences in the visible and near-infrared light region at low temperatures (<50 °C). But ΔT_{sol} of the bilayer film is 8.4% at 50 °C, which indicates that

VO_2/ZnO bilayer film showed a certain phase transition at this temperature. This may be due to the surface defects of ZnO films, such as oxygen vacancy with a shallow energy level which can be excited at low temperature (confirmed by the film resistance-temperature curve in Fig. S1, in which ZnO film showed decreased resistance with increasing the temperature and that is probably due to the increased electrons concentration in the ZnO caused by the thermal excitation of surface defects.) [36], leading to an increase in the electrons in the film and thus a decrease in the solar transmittance of the film. Meanwhile the phase transition process of VO_2 onset at lower temperatures. In addition, ΔT_{sol} of the bilayer film between 20 °C and 90 °C is 16.0%, while that of VO_2 film is 11.3%, which show the enhancement of ΔT_{sol} for bilayer film.

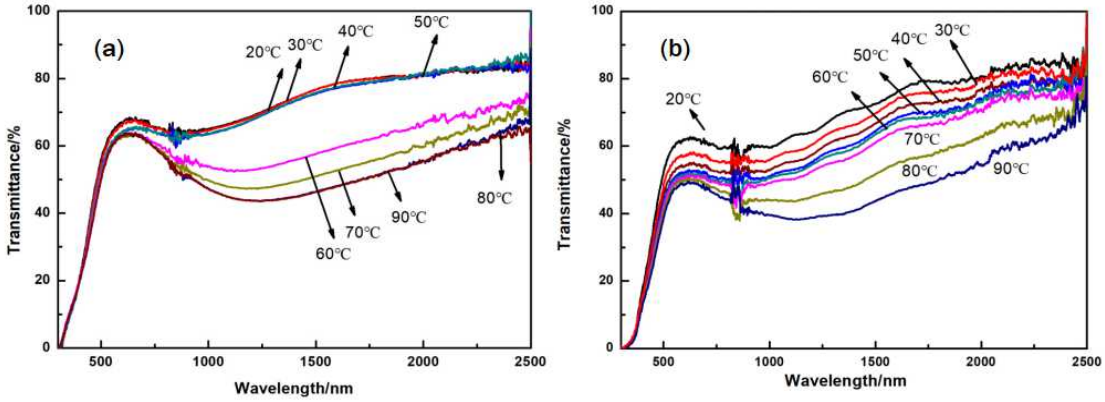

Fig. 4. Transmittance spectra in the range from 300 nm to 2500 nm for (a) VO_2 film and (b) VO_2/ZnO bilayer film at 20 °C and 90 °C.

Table 3 Optical properties of VO_2/ZnO bilayer film and VO_2 film at different temperatures from 20 °C to 90 °C.

Temperature (°C)	VO_2/ZnO bilayer film		VO_2 film	
	T_{lum} (%)	ΔT_{sol} (%)	T_{lum} (%)	ΔT_{sol} (%)
20	58.7	-	63.1	-
30	54.4	3.5	62.2	0.7
40	51.4	6.2	60.4	1.6
50	49.4	8.4	60.6	1.4
60	48.4	9.4	59.0	7.5
70	47.8	10.4	58.4	9.7
80	46.8	13.8	58.6	11.0

90	45.6	16.0	58.5	11.3

3.3. The stability of porous VO_2/ZnO bilayer films

Durability is another important performance of VO_2 film. ZnO can be used as protective layer to prevent the VO_2 from being oxidized to V_2O_5 [21], which can improve the durability of VO_2 film. Herein, VO_2 film and VO_2/ZnO bilayer film were put at ambient temperature and their solar transmittance was measured at 20 °C and 90 °C respectively after 15 days, 40 days, 120 days, 150 days and 300 days. Fig. 5 shows the solar modulation efficiency of VO_2 film and VO_2/ZnO bilayer film dependent on the time. It can be seen that ΔT_{sol} is only 4.1% for VO_2 film after 300 days, indicating a poor stability. This is ascribed to that most VO_2 particles in the film may has been oxidized, which will be confirmed by XPS results later. The solar modulation efficiency remains only 34.3% compared to that of pristine film. However, VO_2/ZnO bilayer film showed almost unchanged ΔT_{sol} of 16.0% after 300 days, suggesting that the bilayer film can prevent the oxidization of VO_2 into V_2O_5 and thus ΔT_{sol} remains 89.9% refer to that of pristine bilayer film. It can also be seen clearly in the inset that the color of VO_2 film is light yellow but the bilayer film is still brown, which indicates an excellent stability of VO_2/ZnO bilayer film. To be noted that there are oxygen vacancies in the ZnO film surface which has been confirmed by the temperature dependent resistance result shown in Figure S1, as the resistance decrease with increasing temperature. And this phenomenon could be assign to the oxygen vacancies with shallow energy level which would be excited by thermal stimulating. The resistance was decreased due to the increased concentration of electrons caused by the thermal excitation of surface defects [36]. And the contact between ZnO layer and VO_2 layer would make the electrons transfer through the interface, leading to the increase of electrons in the VO_2 layer. The transfer electrons not only drive the protons into VO_2 but also enhance the formation energy for oxygen vacancy which is positive charged, thereby delay the oxidization of VO_2 [37-39].

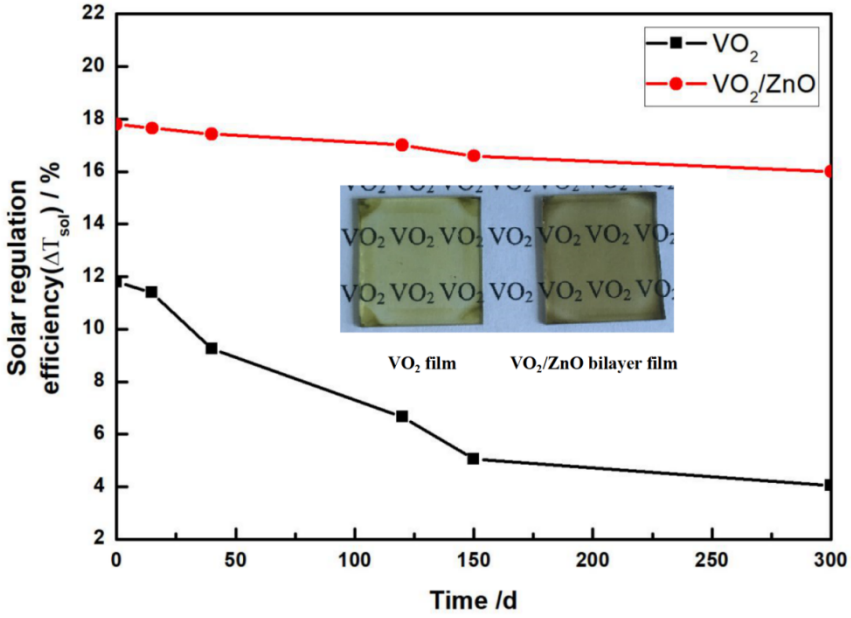

Fig.5. ΔT_{sol} of VO_2 film and VO_2/ZnO bilayer film after 0, 15, 40, 120, 150 and 300 days (the inset shows the photograph of both film (2.5*2.5 cm) after 300 days).

In order to account for the stability of VO_2/ZnO bilayer film, XPS characterization was carried out. Fig. 6 shows the XPS spectra of VO_2 film and VO_2/ZnO bilayer film. The XPS full spectra of both films are shown in Fig. 6a. The signal of C 1s and N 1s peaks come from the PVP in the films. It can be seen that there are Zn, V and O elements in the bilayer film, while V and O elements in the VO_2 film. The Zn core level binding energy was split into Zn $2p_{3/2}$ (1021.5 eV) and Zn $2p_{1/2}$ (1044.6 eV) peaks in Fig. 6d, indicating that there are Zn^{2+} in the bilayer film. The peak of Zn 2p at 1022.5 eV, which corresponding to Zn^{2+} in ZnO [36], indicating that Zn^{2+} exists on the surface of the bilayer film and taking the previous XRD, SEM results into account, the Zn^{2+} may come from the topside uneven ZnO layer because the XPS characterization could only perform into 10 nm deep from the surface. Fig. 6b presents the peaks of V $2p_{3/2}$ and V $2p_{1/2}$ at 515.6 eV and 523 eV, respectively, which are consistent with the peak values of V^{4+} in M-VO_2 as reported in previous works [20,31]. This indicates that the existence of pure M-VO_2 in both bilayer film and VO_2 film. The relative intensity of V 2p peaks are reduced in the bilayer films compared with that in VO_2 film, which is attributed to ZnO that as protective layer with significant peak intensity presented in the film. The peak of O 1s in the bilayer film is shown in Fig. 6c and could be divided into two peaks (530.9 eV and 532.0 eV). The former is assigned to the lattice oxygen from ZnO and VO_2 while the latter belongs to the adsorbed oxygen species on the surface of the top ZnO layer

[21,31,36]. The O 1s peak in VO_2 film can also be divided into two peaks (530.7 eV and 532.3 eV). The peak at 530.7 eV is probably attributed to the lattice oxygen while the other is assigned to adsorbed oxygen on the surface of VO_2 layer. It can be seen that the content of adsorbed oxygen in VO_2 film is lower than that in the bilayer film. This is probably because the top ZnO layer in the bilayer can adsorb more oxygen species.

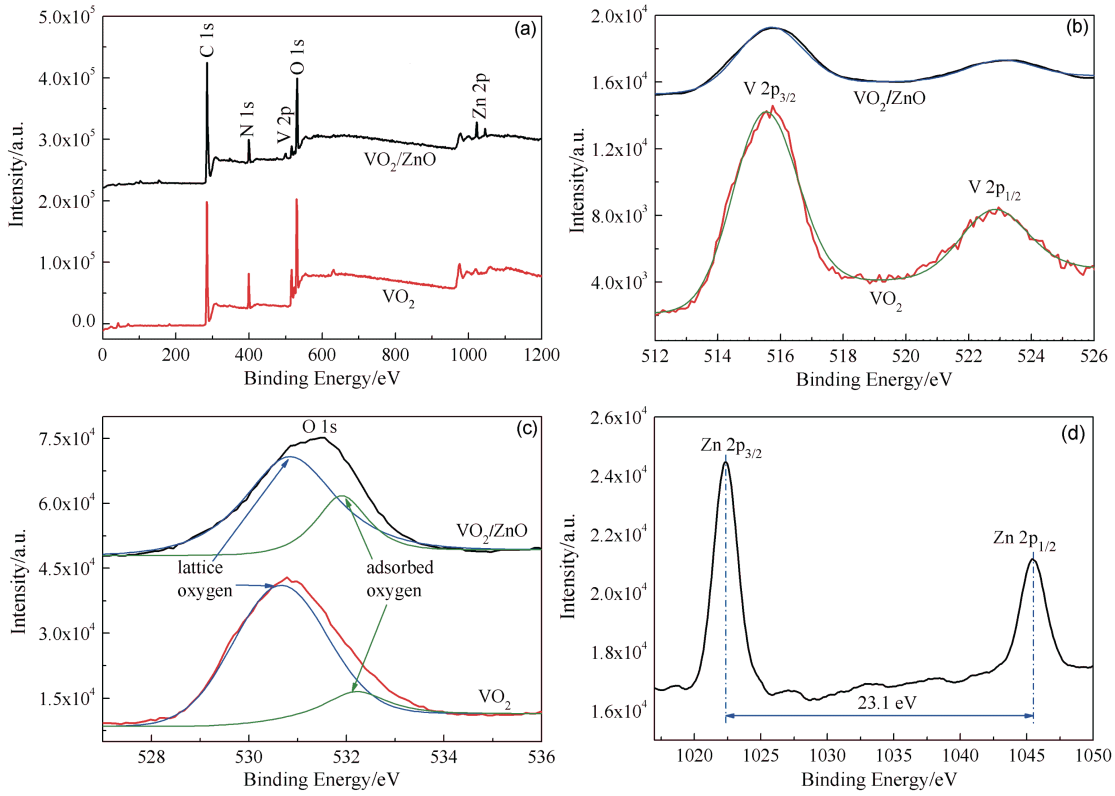

Fig. 6. XPS spectra of (a) survey spectra, (b) V 2p, (c) O 1s from VO_2/ZnO bilayer film and VO_2 film, (d) Zn 2p from VO_2/ZnO bilayer film.

After 300 days, VO_2 thin film and VO_2/ZnO bilayer film were characterized by XPS again and the results are shown in Fig. 7. Fig. 7a shows full spectra of VO_2 thin film and bilayer film. It can be seen that there are C, N, O, V and Zn elements in the bilayer film while C, N, O and V elements in VO_2 film. Except that C and N elements come from the PVP in the films, the bilayer film is still composed of V, Zn and O elements while VO_2 film only includes V and O elements. In Fig. 7b, the peak of V $2p_{3/2}$ in bilayer film was divided into two peaks located at 515.8 eV and 517.0 eV respectively which are corresponding to V^{4+} and V^{5+} [20,31]. The molar ratio of V^{4+} to V^{5+} is 4:1, which is caused by the slow oxidation of VO_2 after long-time exposure to ambient temperature. The content of V_2O_5 is only less than 20%, which indicates the main component of

bilayer film is still M-VO_2. For VO_2 film, the V $2p_{3/2}$ peak was also separated into V^{4+} and V^{5+}, it can be seen that the content of V^{5+} is higher and the molar ratio of V^{4+} to V^{5+} is 1:3, which indicates the most of VO_2 has been oxidized to V_2O_5 due to the poor durability of VO_2 film and leading to the poor solar modulation efficiency. It can be clearly seen that V $2p_{5/2}$ peaks of VO_2 film and VO_2/ZnO bilayer film after 300 days exhibited a large change and can divided into two peaks as shown in Fig. S2. Fig. 7c shows high resolution XPS spectra of O 1s, the peak of O 1s was separated into two peaks: ~530.8 eV and ~532.1 eV. The former belongs to lattice oxygen and the latter is attributed to the adsorbed oxygen as discussed before, which indicates the adsorbed oxygen may still be present in both films. Less adsorbed oxygen existed in the bilayer film than that in VO_2 film, indicating a better durability of the bilayer film. In addition, the content of adsorbed oxygen in the bilayer film decreased while that in the VO_2 film increased significantly after 300 days. Apparently the concentration of adsorbed oxygen varied with the ambient condition and film components. In this work, the durability was not estimated in the constant condition. Thus the results in Figure 6c and 7c obtained from the pristine bilayer film and bilayer film that was preserved for 300 days must be tested under different ambient condition, which was convinced that the concentration of adsorbed oxygen would be affected by the ambient condition especially for temperature. Besides, the densification and aging of PVP in the film surface would also affect the oxygen adsorption process. In this sense, the reason for the variation of concentration of adsorbed oxygen may be assigned to joint factors. Fig. 7d shows the high resolution spectrum of Zn element in the bilayer film. It can be seen that the difference of Zn $2p_{3/2}$ and Zn $2p_{1/2}$ core level binding energy is 23.1 eV, which matches well with the value for Zn^{2+} in ZnO, which indicates that ZnO reminds unchanged (Fig. S3). The results confirm that after putting at ambient temperature for 300 days, the bilayer film is composed of most VO_2, less V_2O_5 and ZnO, while the VO_2 film includes most V_2O_5 and less VO_2. In this sense, the bilayer film exhibited good stability as well as excellent thermochromic performance.

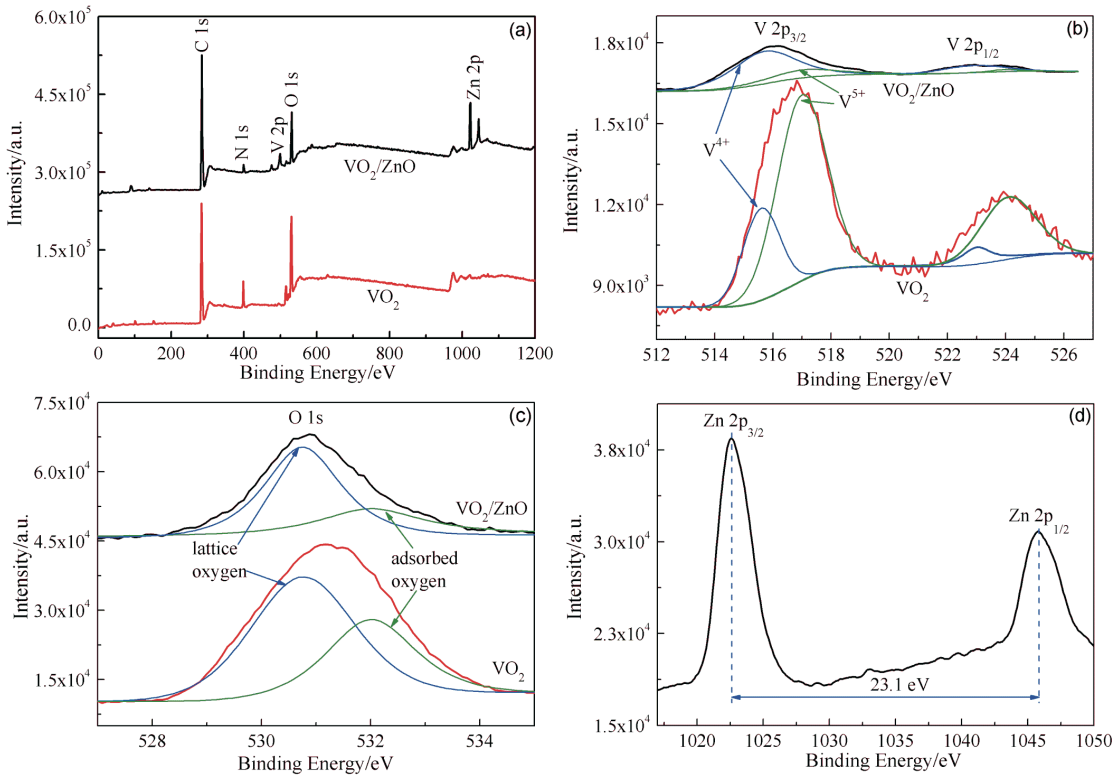

Fig.7. XPS spectra of (a) survey spectra, (b) V 2p, (c) O 1s in VO_2/ZnO bilayer film and VO_2 film after 300 days, (d) Zn 2p in VO_2/ZnO bilayer film after 300 days.

4. Conclusions

In this work, cotton was used as template to synthesize mesoporous VO_2 nanoparticles by hydrothermal method and subsequent thermal treatment, and then VO_2/ZnO bilayer film was prepared by sol-gel method. The obtained bilayer film exhibited excellent thermochromic properties than pure VO_2 film: high visible transmittance of 55.9%, and high solar modulation efficiency of 19.3%. In addition, this bilayer film also exhibited good durability and its solar modulation efficiency are maintained over 16.0% after exposing to ambient conditions for 300 days. This is probably attributed to the presence of protective ZnO layer in the film. In summary, this work can provide a new method to prepare a VO_2-based multilayer film with high thermochromic properties and good durability, which may promote the practical application of VO_2 based film in smart windows.

Acknowledgments

This work was supported by the National Natural Science Foundation of China (Grant No.

51772229), "111" project (No. B18038), the National Key R&D Program of China (No. 2017YFE0192600), and Open Foundation of the State Key Laboratory of Silicate Materials for Architectures at WUT (No. SYSJJ2018-05). We also thank the Analytical and Testing Center of WUT for the help with carrying out XRD, TEM, and FESEM analyses.

References：

[1] M. Kamalisarvestani, R. Saidur, S. Mekhilef, F.S. Javadi, Performance, materials and coating technologies of thermochromic thin films on smart windows, Renew. Sust. Energ. Rev. 26 (2013) 353-364.

[2] C.G. Granqvist, Transparent conductors as solar energy materials: A panoramic review, Solar Energ[J]. Sol. Energ. Mat. Sol. C. 91 (2007) 1529-1598.

[3] R. Zheng, Y. Wang, J. Pan, H.A. Malik, H. Zhang, C. Jia, X. Weng, J. Xie, L. Deng, Towards Easy-to-assemble, Large Area Smart Windows: All-in-one Cross-linked Electrochromic Material and Device, ACS Appl. Mater. Inter. 12 (2020) 27526-27536.

[4] E.S. Lee, D.L. Dibartolomeo, Application issues for large-area electrochromic windows in commercial buildings, Sol. Energ. Mat. Sol. C. 71 (2002) 465-491.

[5] Z. Michele, Office worker preferences of electrochromic windows: A pilot study. Build. Environ. 41 (2006) 1262-1273.

[6] V. Wittwer, M. Datz, J. Ell, A. Georg, W. Graf, G. Walze, Gasochromic windows. Sol. Energ. Mat. Sol. C. 84 (2004) 305-314.

[7] R. Baetens, B.P. Jelle, A. Gustavsen, Properties, requirements and possibilities of smart windows for dynamic daylight and solar energy control in buildings: A state-of-the-art review. Sol. Energ. Mat. Sol. C. 94 (2010) 87-105.

[8] C.M. Lampert, Smart switchable glazing for solar energy and daylight control. Sol. Energ. Mat. Sol. C. 52 (1998) 207-221.

[9] L. Long, H. Ye, How to be smart and energy efficient: A general discussion on thermochromic windows, Sci. Rep. 4 (2014) 6427.

[10] Y. Ke, Y. Y, Q. Zhang, Y. Tan, P. Hu, S. Wang, Y. Tang, Y. Zhou, X. Wei, S. Wu, T.J. White, J. Yin, J. Peng, Q. Xiong, D. Zhao, Y. Long, Adaptive thermochromic windows from active plasmonic elastomers, Joule 3 (2019) 858-871.

[11] J. Zhang, J. Wang, C. Yang, H. Jia, X. Cui, S. Zhao, Y. Xu, Mesoporous SiO_2/VO_2 double-layer thermochromic coating with improved visible transmittance for smart window, Sol. Energy Mater. Sol. C. 162 (2017) 134–141.

[12] F.J. Morin, Oxides which show a metal-to-insulator transition at the Neel temperature, Phys. Rev. Lett. 3 (1959) 34.

[13] Z. Chen, Y. Gao, L. Kang, C. Cao, S. Chen, H. Luo, Fine crystalline VO_2 nanoparticles: synthesis, abnormal phase transition temperatures and excellent optical properties of a derived VO_2 nanocomposite foil, J. Mater. Chem. A. 2 (2014) 2718–2727.

[14] J. Zhu, Y. Zhou, B. Wang, J. Zheng, S. Ji, H. Yao, H. Luo, P. Jin, Vanadium dioxide nanoparticle-based thermochromic smart coating: high luminous transmittance, excellent solar regulation efficiency, and near room temperature phase transition, ACS Appl. Mater. Inter. 7 (2015) 27796–27803.

[15] B. Li, J. Liu, S. Tian, B. Liu, X. Yang, Z. Yu, X. Zhao, VO_2-ZnO composite films with enhanced thermochromic properties for smart windows, Ceram. Int. 46 (2020) 2758-2763.

[16] Wang S, Li C, Tian S, et al. Facile synthesis of VO_2 (D) and its transformation to VO_2 (M) with enhanced thermochromic properties for smart windows, Ceram. Int. 46 (2020) 14739–14746.

[17] X. Cao, N. Wang, J.-Y. Law, S.-C.-J. Loo, S. Magdassi, Y. Long, Nanoporous thermochromic VO_2 (M) thin films: controlled porosity, largely enhanced luminous transmittance and solar modulating ability, Langmuir 30 (2014) 1710–1715.

[18] Z. Tian, B. Xu, B. Hsu, L. Stan, Z. Yang, Y. Mei, Reconfigurable vanadium dioxide nanomembranes and microtubes with controllable phase transition temperatures, Nano Lett. 18 (2018) 3017-3023.

[19] L. Whittaker, C. Jaye, Z. Fu, D.A. Fischer, S. Banerjee, Depressed phase transition in solution-grown VO_2 nanostructures, J. Am. Chem. Soc. 131 (2009) 8884-8894.

[20] B. Li, S. Tian, H. Tao, X. Zhao, Tungsten doped M-phase VO_2 mesoporous nanocrystals with enhanced comprehensive thermochromic properties for smart windows, Ceram. Int. 45 (2019) 4342-4350.

[21] H. Zhou, J. Li, S. Bao, J. Li, X. Liu, P. Jin, Use of ZnO as antireflective, protective, antibacterial, and biocompatible multifunction nanolayer of thermochromic VO_2 nanofilm for intelligent windows, Appl. Surf. Sci. 363 (2016) 532–542.

[22] K. Tong, R. Li, H. Yao, H. Zhou, X. Zeng, S. Ji, P. Jin, Preparation of VO_2/Al-O core-shell structure with enhanced weathering resistance for smart window, Ceram. Int. 43 (2017) 4055-4061.

[23] Y. Gao, S. Wang, H. Luo, L. Dai, C. Cao, Y. Liu, Z. Chen, M. Kanehira, Enhanced chemical stability of VO_2 nanoparticles by the formation of SiO_2/VO_2 core/shell structures and the application to transparent and flexible VO_2-based composite foils with excellent thermochromic properties for solar heat control, Energy Environ. Sci. 5 (2012) 6104–6110.

[24] J. Parker, Raman scattering from VO_2 single crystals: a study of the effects of surface oxidation, Phys. Rev. B 42 (1990) 3164.

[25] X. Cao, T. Chang, Z. Shao, F. Xu, H. Luo, P. Jin, Challenges and Opportunities Toward Real Application of VO_2-Based Smart Glazing, Matter 2 (2020) 862-881.

[26] Y. Wang, F. Zhao, J. Wang, A.R. Khan, Y. Shi, Z. Chen, K. Zhang, L. Li, Y. Gao, X. Guo, VO_2@SiO_2/poly (n-isopropylacrylamide) hybrid nanothermochromic microgels for smart window, Ind. Eng. Chem. Res. 57 (2018) 12801-12808.

[27] M. Wang, J. Tian, H. Zhang, X. Shi, Z. Chen, Y. Wang, A. Ji, Y. Gao, Novel synthesis of pure VO_2@SiO_2 core@ shell nanoparticles to improve the optical and anti-oxidant properties of a VO_2 film, RSC Advances 6 (2016) 108286-108289.

[28] Y. Li, S. Ji, Y. Gao, H. Luo, M. Kanehira, Core-shell VO_2@TiO_2 nanorods that combine

thermochromic and photocatalytic properties for application as energy-saving smart coatings. Sci. Rep. 3 (2013) 1370.

[29] Y. Chen, X. Zeng, J. Zhu, R. Li, H. Yao, X. Cao, S. Ji, P. Jin, High performance and enhanced durability of thermochromic films using VO_2@ZnO core–shell nanoparticles, ACS Appl. Mater. Inter. 9 (2017) 27784-27791.

[30] S. Zhao, Y. Tao, Y. Chen, Y. Zhou, R. Li, L. Xie, A. Huang, P. Jin, S. Ji, Room temperature synthesis of inorganic-organic hybrid coated VO_2 nanoparticles for enhanced durability and flexible temperature-responsive near-infrared modulator application. ACS Appl. Mater. Inter. 11 (2019) 10254–10261.

[31] S. Wu, S. Tian, B. Liu, H. Tao, X. Zhao, R.G. Palgrave, G. Sankar, I.P. Parkin, Facile synthesis of mesoporous VO_2 nanocrystals by a cotton-template method and their enhanced thermochromic properties, Sol. Energ. Mat. Sol. C. 176 (2018) 427-434.

[32] S. Tian, Q. Liu, J. Sun, M. Zhu, S. Wu, X. Zhao, Mesoporous ZnO nanorods array with a controllable area density for enhanced photocatalytic properties, J. Colloid Interf. Sci. 534 (2019) 389–398.

[33] B. Zhuang, Z. Dai, S. Pang, H. Xu, L. Sun, F. Ma, 3D Ordered Macroporous VO_2 Thin Films with an Efficient Thermochromic Modulation Capability for Advanced Smart Windows, Adv. Opt. Mater. 7 (2019) 1900600.

[34] S. Dou, J. Zhao, W. Zhang, H. Zhao, F. Ren, L. Zhang, X. Chen, Y. Zhan, Y. Li, A universal approach to achieve high luminous transmittance and solar modulating ability simultaneously for vanadium dioxide smart coatings via double-sided localized surface plasmon resonances, ACS Appl. Mater. Inter. 12 (2020) 7302-7309.

[35] B. Li, J. Yao, S. Tian, Z. Fang, S. Wu, B. Liu, X. Gong, H. Tao, X. Zhao. A facile one-step annealing route to prepare thermochromic W doped VO_2 (M) particles for smart windows, Ceram. Int. 46 (2020) 18274-18280.

[36] X. Zhang, J. Qin, Y. Xue, P. Yu, B. Zhang, L. Wang, R. Liu, Effect of aspect ratio and surface defects on the photocatalytic activity of ZnO nanorods, Sci. Rep. 4 (2014) 4596.

[37] Y. Chen, Z. Wang, S. Chen, H. Ren, L. Wang, G. Zhang, Y. Lu, J. Jiang, C. Zou, Y. Luo, Non-Catalytic Hydrogenation of VO_2 in Acid Solution, Nat. Commun. 9 (2018) 818.T. https://doi.org/10.1038/s41467-018-03292-y

[38] S. Chen, Z. Wang, H. Ren, Y. Chen, W. Yan, C. Wang, B. Li, J. Jiang, C. Zou, Gate-Controlled VO_2 Phase Transition for High Performance Smart Windows, Sci. Adv. 5 (2019) eaav6815. https://doi.org/ 10.1126/sciadv.aav6815

[39] Y. Chen, Z. Shao, Y. Yang, S. Zhao, Y. Tao, H. Yao, H. Luo, X. Cao, P. Jin, Electrons-Donating Derived Dual-Resistant Crust of VO_2 Nano-Particles via Ascorbic Acid Treatment for Highly Stable Smart Windows Applications, ACS Appl. Mater. Interfaces 11 (2019) 41229−41237. https://doi.org/ 10.1021/acsami.9b11142

Supporting information

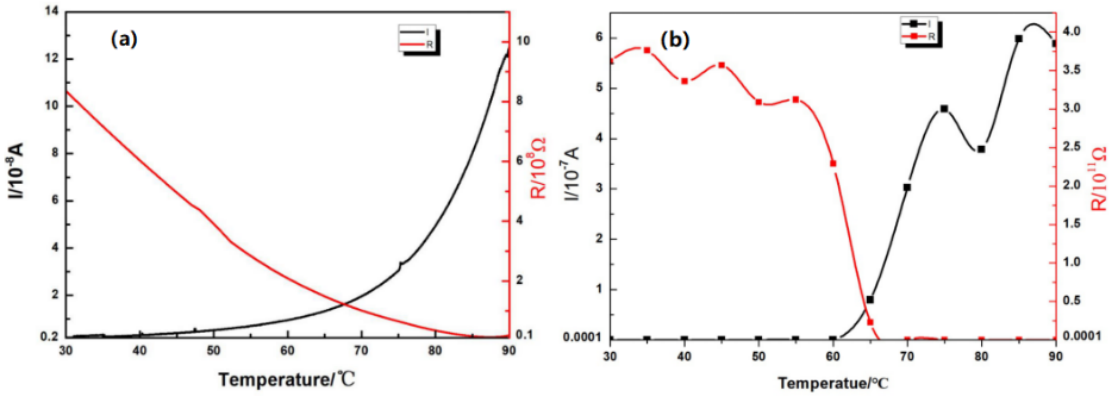

Fig. S1. Current and Resistance changes of ZnO film and VO_2/ZnO bilayer film at different temperatures from 30 °C to 90 °C.

Fig. S1 shows the I-T and R-T curves of VO_2/ZnO bilayer film and ZnO film. In the test, the voltage applied on both ends of the film being kept constant and the temperature is raised slowly and the results are shown in Fig. S1. Fig. S1a shows the current (I) and resistance (R) of the ZnO film with increasing temperature. It can be seen that the current of the ZnO thin film increases with increasing temperature, while the resistance decreases gradually. It was reported that most of ZnO films prepared in the laboratory are n-type semiconductors with donor defects [S1], and the oxygen vacancies are present as a major component. It was reported that the oxygen vacancies are positively correlated with the content of adsorbed oxygen [S2]. With increasing temperature, the electrons bound by donor defects will be excited into the conduction band, resulting in an increase in the concentration of electrons in ZnO layer. Therefore, the film current increases and resistance decreases with increase in temperature. Fig. S1b shows the electrical characteristics of VO_2/ZnO bilayer film. It can be seen that the current intensity of bilayer film exhibits a sharp rise near 60 °C, and the resistance begin to decline rapidly at 55 °C, which implies the insulator-metal phase transition of bilayer film occurred at ca 55 °C to 60 °C, which is lower than that of pure VO_2 film. Combining with XPS results in Fig. 6c, it is found that, from O 1s spectrum, the O-H content is higher, which means more oxygen vacancies in ZnO layer, with the increase of temperature, more electrons in the donor level of ZnO defect are excited into the conduction band, thus increasing the electrons concentration in the conduction band, and some electrons are transferred to VO_2 film, which increased electron density of VO_2 thin film which would affect the phase transition process

of VO_2 significantly [S3], resulting in a decline in the solar transmittance of the bilayer film.

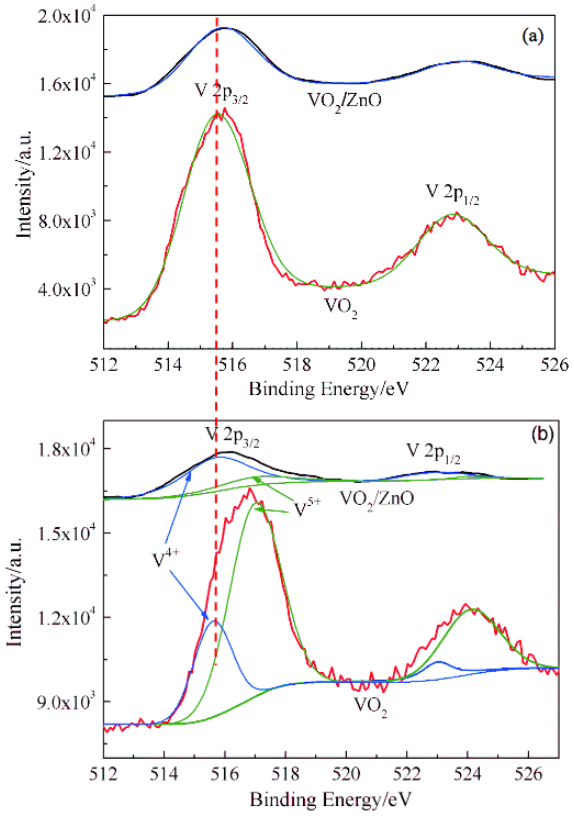

Fig. S2. XPS spectra of V 2p of VO_2 film and VO_2/ZnO bilayer film: (a)pristine, (b) after 300 days.

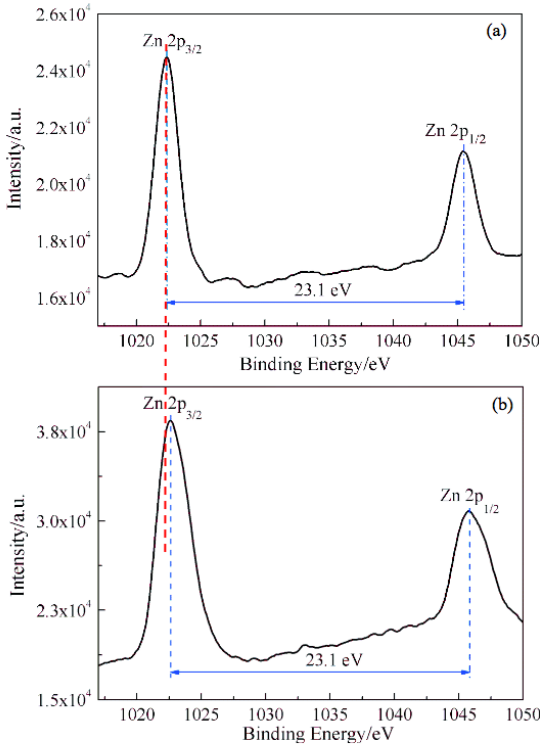

Fig.S3. XPS spectra of Zn 2p of VO_2/ZnO bilayer films: (a) pristine, (b) after 300 days.

Reference

[S1] Z. Xiao, Y. Liu, J. Zhang, D. Zhao, Y. Lu, D. Shen, X. Fan, Electrical and structural properties of *p*-type ZnO: N thin films prepared by plasma enhanced chemical vapour deposition, Semicond. Sci. Tech. 20 (2005) 796.

[S2] Z. Wang, H. Jia, T. Zheng, Y. Dai, C. Zhang, X. Guo, T. Wang, L. Zhu, Promoted catalytic transformation of polycyclic aromatic hydrocarbons by MnO_2 polymorphs: Synergistic effects of Mn^{3+} and oxygen vacancies, Appl. Catal. B-Environ. 272 (2020) 119030.

[S3] R.M. Wentzcovitch, W.W. Schulz, P.B. Allen, VO_2: Peierls or Mott-Hubbard? A view from band theory, Phys. Rev. let. 72 (1994) 3389-3392.